Available online at www.sciencedirect.com

ScienceDirect

Energy Procedia 114 (2017) 5748 – 5760

Energy Procedia

13th International Conference on Greenhouse Gas Control Technologies, GHGT-13, 14-18 November 2016, Lausanne, Switzerland

Geologic carbon storage for shale gas recovery

Oscar Molina[a], Victor Vilarrasa[b,c], Mehdi Zeidouni[a]*

[a]*Dept of Petroleum Engineering, Louisiana State University, Baton Rouge, LA 70803, USA*
[b]*Laboratory of Soil Mechanics, École Polytechnique Fédérale de Lausanne, CH-1015 Lausanne, Switzerland*
[c]*Institute of Environmental Assessment and Water Research, Spanish National Research Council (IDAEA-CSIC), 08034 Barcelona, Spain*

Abstract

We consider the feasibility of a novel Carbon Capture, Utilization and Storage (CCUS) concept that consists in producing oil and gas from hydrocarbon-rich shales overlying deep saline aquifers that are candidates for CO_2 storage. Such geological overlapping between candidate aquifers for CO_2 storage and shale plays exists in several sedimentary basins across the continental US. Since CO_2 reaches the storage formation at a lower temperature than the in-situ temperature, a thermal stress reduction occurs, which may lead to hydraulic fracturing of the caprock overlying the aquifer. In this work, we use a thermo-hydro-mechanical approach for modelling a caprock-aquifer-baserock system. We show that hydraulic fracturing conditions are induced within the aquifer by thermal stress reduction caused by cooling and that hydraulic fractures eventually propagate into the lower portion of the shale play. Nonetheless, fracture height of penetration in the caprock is considerably short after 10 years of injection, so the overall caprock sealing capacity is maintained. To maximize the benefit of the proposed CCUS method, CO_2 injection should be maintained as long as possible to promote the penetration depth of cooling-induced hydraulic fractures into organic-rich shales. Though drilling a horizontal well in the lower portion of the shale to produce hydrocarbons from the induced hydraulic fractures may not be technically feasible, hydrocarbons can still be produced through the injection well. The production of hydrocarbons at the end of the CO_2 storage project will partly compensate the costs of CCS operations.

Peer-review under responsibility of the organizing committee of GHGT-13.

Keywords: cold CO_2 injection; hydraulic fracturing; caprock damage; geomechanics; organic-rich shales

* Corresponding author. Tel.: +1-225-578-8144; fax: +1-888-965-9518.
E-mail address: zeidouni@lsu.edu

Peer-review under responsibility of the organizing committee of GHGT-13.
doi:10.1016/j.egypro.2017.03.1713

1. Introduction

Carbon Capture and Sequestration (CCS) has been recognized in recent years as a potential method to mitigate greenhouse gases emissions. However, one of the most restrictive drawbacks of CCS is its cost of implementation at large scale [1]. Therefore, finding ways to utilize carbon dioxide (CO_2) can improve the economics of CCS projects. A variety of methods for Carbon Capture, Utilization and Storage (CCUS) have been proposed. For instance, Randolph and Saar [2] proposed the CO_2-plume geothermal (CPG) technology as a feasible application of CCUS in which CO_2 is used as the working fluid to recover geothermal energy from deep geological formations. Also, CO_2 Enhanced Oil Recovery (CO_2 EOR) has been successfully used in the oil industry for more than 40 years. Moreover, technologies used in CO_2 EOR are similar to those sought after in CCS, which can be beneficial for the successful deployment of CCS projects (e.g., [3]). Nevertheless, more CCUS methods are required to convert CCS in an economically feasible option to significantly reduce CO_2 emissions.

We propose a novel CCUS concept that seeks to take advantage of the fact that CO_2 reaches the bottom of injection wells at a lower temperature than that of the storage formation [4, 5]. Since cooling induces a thermal stress reduction, the minimum effective stress may become lower than the tensile strength of the rock for large temperature decrease and/or in stiff rocks, which would form hydraulic fractures through which hydrocarbons could be recovered. Several authors have investigated the impact of cold CO_2 on the geomechanical integrity of the caprock as well as its sealing performance [e.g., 5, 6]. Preisig and Prévost [7], for instance, performed fully coupled simulations of CO_2 injection at different temperatures into a saline aquifer through a horizontal well based on the CCS site at In Salah, Algeria. Preisig and Prévost [7] found that tensile stresses can indeed develop in the caprock due to thermal stresses. A separate study by Gor et al. [8] supports the former claim. Gor et al. [8] found that the time at which tensile stresses develop in the caprock depends not only on the injection temperature, but also on the magnitude of the initial stress field and the injection pressure. Vilarrasa et al. [5] studied cold (liquid) CO_2 injection in a deep saline aquifer overlaid and underlain by shale layers. They found that rock contracts within the cold front inside the reservoir, yielding a reduction in total stresses in all directions. Nonetheless, stresses are redistributed and the caprock-aquifer interface gets actually tightened during the first months of injection. Interestingly, all these studies indicate that for a sufficiently long CO_2 injection, cooling will propagate into the lower portion of the caprock and tensile stresses may develop, which could form hydraulic fractures through which shale oil and/or gas could be produced.

The goal of this study is to investigate the feasibility of this novel CCUS concept based on producing hydrocarbons from organic-rich shales overlying deep saline aquifers suitable for CCS through hydraulic fractures formed as a result of the cooling induced by CO_2 injection. To this end, we assess rock cooling effects on in-situ stresses for a cold CO_2 injection process performed in a caprock-aquifer-baserock configuration through the numerical solution of coupled geomechanics, heat transfer and fluid mechanics, i.e., thermo-hydro-mechanical (THM), simulations. We first describe the concept of the proposed CCUS method in Section 2.1. The remaining of this paper is focused on examining whether the proposed method for producing hydrocarbons from the overlying shale layer is geologically and physically sound. The feasibility of finding a geologic setting such that a deep saline aquifer candidate for CO_2 is indeed overlaid by an organic-rich shale is discussed in Section 2.2. Section 3 presents the mathematical formulation, modeling and numerical simulation of the coupled THM phenomenon aiming to predict the occurrence of hydraulic fracturing of the caprock-aquifer interface and the shale layer due to thermal effects. Section 4 presents THM simulation results for the proposed cold CO_2 injection case study. Finally, we draw some conclusions on the feasibility of the proposed CCUS method.

Nomenclature

$\mathbf{b}$	Vector of body forces $[ML^{-2}T^{-2}]$
c_r	Rock compressibility factor $[M^{-1}LT^{2}]$
D	Depth [L]
E	Young's modulus $[ML^{-1}T^{-2}]$
α	Phase index, c refers to the CO_2 rich phase and w to aqueous phase
h_α	Enthalpy of phase α $[ML^{2}T^{-2}]$
$\mathbf{I}$	Identity matrix $[-]$

$\mathbf{j}_s$	Flux of solid phase $[ML^{-2}T^{-1}]$
k	Absolute permeability $[L^2]$
$k_{r\alpha}$	Relative permeability of phase α $[-]$
p	Pressure $[ML^{-1}T^{-2}]$
p_α	Pressure of phase α $[ML^{-1}T^{-2}]$
$\mathbf{q}_\alpha$	Volumetric flux of phase α $[L^3L^{-2}T^{-1}]$
r_α	Source/sink of phase α $[ML^{-3}T^{-1}]$
S_α	Saturation of phase α $[-]$
t	Time $[T]$
T	Absolute temperature $[\Theta]$
$\mathbf{u}$	Displacement vector $[L]$
α_T	Coefficient of thermal expansion $[\Theta^{-1}]$
β	Biot coefficient $[-]$
Δp	Pressure differential $[ML^{-1}T^{-2}]$
ΔT	Temperature differential $[\Theta]$
$\boldsymbol{\varepsilon}$	Strain tensor $[LL^{-1}]$
ϕ	Porosity $[-]$
ϕ'	Friction angle $[-]$
λ	Thermal conductivity $[MLT^{-3}\Theta^{-1}]$
μ_α	Viscosity of phase α $[ML^{-1}T^{-1}]$
ν	Poisson ratio $[-]$
∇	Gradient operator $[L^{-1}]$
ρ_α	Density of phase α $[ML^{-3}]$
$\boldsymbol{\sigma}$	Stress tensor of the rock matrix $[ML^{-1}T^{-2}]$
$\boldsymbol{\sigma}_0$	Initial principal stresses at depth D $[ML^{-1}T^{-2}]$
σ'_h	Minimum horizontal effective stress $[ML^{-1}T^{-2}]$
σ_{ob}	Overburden stress $[ML^{-1}T^{-2}]$

2. CCUS Method for Shale Gas Production

2.1. The concept of the proposed CCUS method

Basically, we aim to take advantage of rock cooling effects to allow tensile stresses to appear in the caprock, which would allow hydraulic fracture propagation from the aquifer into the caprock due to the cooling-induced thermal stress reduction (Fig. 1). The change in stress state is mainly due to the difference between the temperature of the injected fluid and the in-situ temperate, which ultimately yields a reduction of thermal stresses in the cooled region located near the CO_2 injection well and the caprock-aquifer interface. As a result of the hydraulic fractures formation, hydrocarbons from the shale play that acts as a caprock could be extracted once CO_2 injection finishes. To produce hydrocarbons, the same horizontal injection well used for injection can be used once the projected CO_2 volume for storage has been put in place. This option has the considerable financial advantage of avoiding drilling an additional horizontal well in the shale layer. An alternative possibility would be to drill another horizontal well across the hydraulic fractures within the shale layer through which hydrocarbons are produced. At this point, the injection well should be shut-in or plugged-in and abandoned, so that the production well becomes the only fully operational well in the process (see Fig. 1). Overall, our methodology is based on the premise that long-term thermal effects due to cold CO_2 injection into saline aquifers would allow the development of hydraulic fractures that will allow the production of shale oil and/or gas.

Since CO_2 actually reaches the bottom of the injection well at a temperature lower than that of the host rock, we foresee that our proposed CCUS methodology could be deployed without any additional action during the injection process because cooling of the subsurface is a natural consequence of CCS. Indeed, the temperature difference can become quite considerable, e.g., 45°C at In Salah [9, 10] and 51°C at Cranfield, Mississippi [11]. Given these high

temperature differences, if a horizontal CO_2 injection well is drilled near the caprock-aquifer interface, we anticipate the occurrence of tensile fractures in the caprock after several years of CO_2 injection. Once the CO_2 injection phase finishes, hydrocarbons could be produced through the formed hydraulic fractures. Similar to CO_2 EOR, the drawback of the proposed CCUS method would be the production of part of the injected CO_2 along with the produced hydrocarbons, but this extracted CO_2 could be reinjected together with the CO_2 emitted by the produced hydrocarbons. However, advantages overcome limitations: the costs of CCS would be compensated by hydrocarbon production, no extra energy is required to form the hydraulic fractures and the need for use of water for fracturing is eliminated.

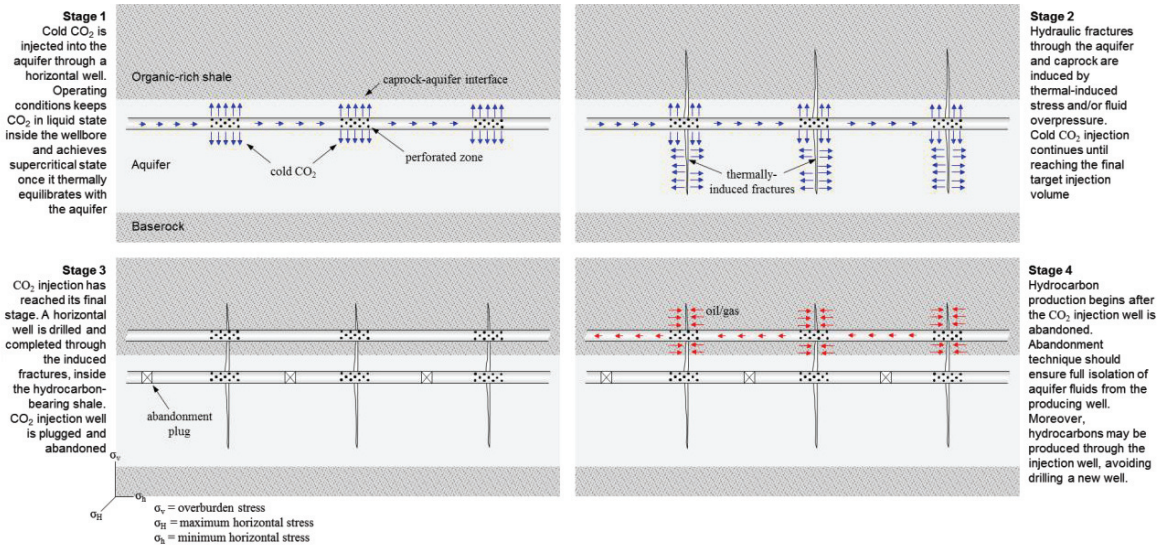

Fig. 1—Schematics of the proposed CCS/shale gas production methodology

2.2. Feasibility of the hydrocarbon-bearing shale-aquifer configuration

To assess the feasibility of the proposed CCUS method, it is necessary to investigate the existence of deep saline aquifers suitable for CCS projects which are overlaid by hydrocarbon-bearing shales. Elliot and Celia [12] suggested that such geological configuration actually occurs across the U.S. Fig. 2 illustrates the geographic overlapping existing between continental producing shales or tight gas plays and potential deep saline aquifers candidates for CCS in the continental U.S. This map was obtained by combining data from the U.S. Energy Information Administration (EIA) (http://www.eia.gov) for producing shales and the National Carbon Sequestration Database and Geographic Information System (NATCARB) (http://natcarb.netl.doe.gov/) for identifying the potential aquifers suitable for CCS projects.

Nevertheless, caution must be used since the study from Elliot and Celia [12] did not take into consideration the vertical geologic profile. Hence, Fig. 2a should be used as a "first-cut areal analysis" for determining the suitability of the selection of a certain location for implementing the proposed CCUS method. Therefore, the concept of injecting cold CO_2 in a deep saline aquifer overlaid by an organic-rich shale seeking to produce oil and/or gas by inducing hydrofractures that penetrate into the lower portion of the caprock, either by hydraulic fracturing or reactivation of preexisting fractures, seems at least geologically feasible.

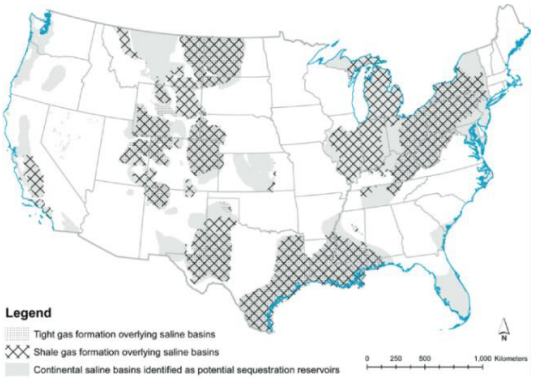

(a) potential zones for CO_2 injection and producing shales overlapping map (from Elliot and Celia [12])

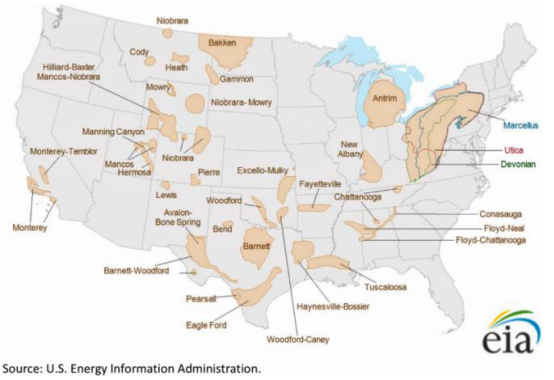

(b) location of shale plays in the U.S. lower 48 states (source: U.S. Energy Information Administration–EIA)

Fig. 2—(a) Overlapping map and (b) shale plays across the continental U.S.

3. Mathematical Modeling

3.1. Thermo-hydro-mechanical modeling formulation

The process of injecting CO_2 into a deep saline aquifer at a lower temperature than that of the aquifer itself, whose average temperature is given by the in-situ geothermal gradient, induces changes in the stress state of the rock layers composing the geologic storage system, i.e., aquifer and overlying shale. To predict such changes and their implication on the caprock mechanical sealing performance, it is necessary to setup a mathematical model in which conservation laws are simultaneously acting upon the fluid, composed by CO_2 ($\alpha = c$) and interstitial water ($\alpha = w$), and solid phases, composed by sandstone (aquifer) and shales (caprock and baserock). The mass conservation law for the fluid phase is mathematically expressed as [13]

$$\frac{\partial}{\partial t}(\phi S_\alpha \rho_\alpha) + \nabla \cdot (\rho_\alpha \mathbf{q}_\alpha) = r_\alpha \ , \tag{1}$$

where ϕ [–] is the porosity of the medium, S_α [–] is saturation of the α phase, ρ_α [ML^{-3}] is the α phase density, $\mathbf{q}_\alpha$ [LT^{-1}] is the volumetric flux of the α phase, r_α [$ML^{-3}T^{-1}$] represents phase change of fluid α, and t [T] is time. For simplicity, we assume that CO_2 evaporation into the water phase is negligible. We use Darcy's law as the momentum conservation law for the fluid phase,

$$\mathbf{q}_\alpha = -\frac{k k_{r\alpha}}{\mu_\alpha}(\nabla p_\alpha + \rho_\alpha g \nabla D) \, , \tag{2}$$

where k [L^2] is the intrinsic permeability of the rock matrix, $k_{r\alpha}$ [–] is the relative permeability to the α phase, μ_α [$ML^{-1}T^{-1}$] is the viscosity of the α phase, p_α [$ML^{-1}T^{-2}$] is the pressure of the α phase, g [LT^{-2}] is the gravity acceleration and D [L] is the depth with respect to the datum level. In addition, the energy conservation law for both fluid and solid phases is expressed as [14]

$$\frac{\partial}{\partial t}[(1-\phi)\rho_s h_s + \phi(\rho_w S_w h_w + \rho_c S_c h_c - S_w p_w - S_c p_c)] + \nabla \cdot (-\lambda \nabla T + \rho_w h_w \mathbf{q}_w + \rho_c h_c \mathbf{q}_c) = 0 \, , \tag{3}$$

where ρ_s [$\mathrm{ML^{-3}}$] is the solid phase density, h_α [$\mathrm{ML^{-2}T^{-2}}$] is enthalpy of both fluid and solid phases, λ [$\mathrm{MLT^{-3}\Theta}$] is thermal conductivity of the rock and T [Θ] is absolute temperature. An important assumption made herein is that all phases are in thermal equilibrium at any point of the domain during the injection process.

For the mechanical problem, we need to solve the momentum conservation for the solid phase. If we neglect inertial effects, momentum equation of the solid phase reduces to the equation of equilibrium of stresses

$$\nabla \cdot \boldsymbol{\sigma} + \mathbf{b} = \mathbf{0}, \tag{4}$$

where $\boldsymbol{\sigma}$ [$\mathrm{ML^{-1}T^{-2}}$] is the stress tensor and $\mathbf{b}$ [$\mathrm{ML^{-2}T^{-2}}$] is the vector of body forces acting upon the solid phase. Under the assumption of an elastic medium, i.e., thermoelasticity, elastic strain is a function of total stresses, overpressure and temperature as [15]

$$\boldsymbol{\varepsilon} = \frac{1+\nu}{E}\boldsymbol{\sigma} - \frac{\nu}{E}(\sigma_{xx}+\sigma_{yy}+\sigma_{zz})\mathbf{I} - \left(\frac{1-2\nu}{E}\Delta p - \alpha_T \Delta T\right)\mathbf{I}, \tag{5}$$

where $\boldsymbol{\varepsilon}$ [$\mathrm{LL^{-1}}$] is the strain tensor, ν [–] is Poisson ratio, E [$\mathrm{ML^{-1}T^{-2}}$] is the Young's modulus, $\mathbf{I}$ [–] is the identity matrix, $\sigma_{ii} \mid i \in (x,y,z)$ [$\mathrm{ML^{-1}T^{-2}}$] represents the stresses over each orthogonal Cartesian direction, $\Delta p = p - p_0$ [$\mathrm{ML^{-1}T^{-2}}$] is fluid overpressure, with $p = \max(p_0, p_c)$, p_0 is the initial hydrostatic pressure, and $\Delta T = T_c - T_0$ [Θ] is the difference between the temperature of the injected CO_2, T_c, and the initial in-situ temperature, T_0.

Equation (5) indicates that the stress state of the rock matrix depends on both pressure and temperature, so that changes in either pore pressure or temperature can ultimately induce rock deformation. Since rock matrix is a deformable medium, porosity must also change. Using the mass conservation law for the solid phase we get

$$\frac{\partial}{\partial t}\left[(1-\phi)\rho_s\right] + \nabla \cdot \mathbf{j}_s = 0, \tag{6}$$

where $\mathbf{j}_s$ [$ML^{-2}T^{-1}$] is the flux of solid phase, given by

$$\mathbf{j}_s = (1-\phi_s)\rho_s \frac{d\mathbf{u}}{dt}, \tag{7}$$

where $\mathbf{u} = (u_x, u_y, u_z)$ [L] is the displacement vector. Equations (6) and (7) can be put together by making use of the definition of material derivative to obtain a general expression for porosity variation that reads [5]

$$\frac{D\phi}{Dt} = \left(\frac{1-\phi}{\rho_s}\right)\frac{D\rho_s}{Dt} + (1-\phi)\nabla \cdot \frac{d\mathbf{u}}{dt}. \tag{8}$$

Finally, if both solid isothermal compressibility c_r [$\mathrm{M^{-1}LT^2}$] and thermal expansion coefficient α_s [Θ^{-1}] are assumed invariant with changes in pressure and temperature, the solid phase density can be expressed, with respect to a reference density ρ_{s0} evaluated at (p_0, T_0), using the following equation of state (EOS)

$$\rho_s = \rho_{s0} \exp\left[c_r(p-p_0) - \alpha_T(T-T_0)\right]. \tag{9}$$

The term $c_r(p-p_0)$, which controls changes in density due to changes in pore pressure, is negligible because compressibility of solid grains is much smaller than bulk compressibility. Therefore, the solid density changes mainly due to temperature changes. Henceforth, $\rho_s = \rho_{s0}\exp[-\alpha_T(T-T_0)]$.

3.2. Stress state of the rock

We assume that the geological system under study is found in a normal faulting stress regime. Hence, the maximum stress is the vertical stress, and is given by the overburden gradient. By assuming a grain density of $2650\ \text{kg/m}^3$, the overburden stress gradient results in $\nabla\sigma_{ob} = 0.026$ MPa/m. Furthermore, hydrostatic pressure gradient is $\nabla p_w = 0.0103$ MPa/m. The initial minimum in-situ horizontal stress is computed using the following equation [16]

$$\nabla\sigma_h = \frac{\nu}{1-\nu}(\nabla\sigma_{ob} - \beta\nabla p_w) + \beta\nabla p_w, \tag{10}$$

where β [–] is the Biot coefficient and is assumed to equal 1 [16]. In the expression above, tectonic stresses and in-situ temperature gradient effects have been neglected. We consider horizontal stresses initially equal in all horizontal directions. Therefore, initial principal stresses at any given depth D [L] are given by the vector

$$\boldsymbol{\sigma}_0 = (\nabla\sigma_{ob}, \nabla\sigma_h, \nabla\sigma_h)\times D. \tag{11}$$

3.3. Hydraulic fracturing

Hydraulic fracturing is initiated if the pore pressure exceeds the sum of the minimum in-situ horizontal stress plus the tensile strength of the formation. A more conservative assumption would be to neglect the tensile strength, allowing for a safety margin of fluid overpressure [17]. Consequently, the fluid pressure to initiate a fracture with no tensile strength is $p \geq \sigma_h$. Since the minimum horizontal effective stress is $\sigma'_h = \sigma_h - p$, a hydraulic fracture would be initiated if

$$\sigma'_h \leq 0. \tag{12}$$

Poisson ratio of shales is usually larger than that of a medium to hard sandstone (Table 1). As a result, according to Equation (10), the horizontal stresses tend to be lower in sandstone than in shale. Thus, hydraulic fracturing of the aquifer would occur first and the fracture will propagate horizontally across the sandstone while fracture height grow is contained by the underlying and overlying shales. However, fracture would start growing vertically through the caprock if the difference in minimum in-situ horizontal stresses between the aquifer rock and the caprock is equal or greater than the net pore pressure, $\Delta\sigma_h \geq p - \sigma_h$ with $\Delta\sigma_h = (\sigma_h)_{\text{shale}} - (\sigma_h)_{\text{aquifer}}$ evaluated at the caprock-aquifer interface depth. In practice, a typical value of $\Delta\sigma_h = 0.7(p-\sigma_h)$ is used to avoid uncontained fracture height grow through shale layers during hydraulic fracturing jobs [16]. Here, we assume that both shale and sandstone have the same Poisson ratio ($\nu = 0.3$), which is a conservative assumption because the likelihood of vertical fracture grow through the shale layer increases given that the aquifer becomes fractured during the injection process. Notice that the sign convention in [15] opposes such of geomechanics due to the fact that this area deals with pore pressure (action) which sees a resistance from the rock (stress state, reaction).

Table 1. Typical range for Young's modulus and Poisson ratio for different types of rock [16]

Lithology	Young's modulus (GPa =1 ×10^3 MPa)	Poisson ratio (–)
Soft sandstone	0.7 – 6.9	0.2 – 0.35
Medium sandstone	13.8 – 34.5	0.15 – 0.25
Hard sandstone	41.4 – 68.9	0.1 – 0.15
Limestone	55.1 – 82.7	0.3 – 0.35
Coal	0.7 – 6.9	0.35 – 0.45
Shale	6.9 – 68.9	0.28 – 0.43

3.4. Numerical simulation

We model a plane strain 2-D caprock-aquifer-baserock system where cold CO_2 is injected at near-critical conditions ($p_{cr} = 15$ MPa, $\Delta T = 33$°C) (Fig. 3). The top of the 100-m thick caprock is placed at 914.4-m deep. The aquifer is 20-m thick and is followed downward by a layer of shale (baserock) with a thickness of 100 m (Table 2). CO_2 is injected through a horizontal well placed 2 m below the caprock-aquifer interface.

We assume a geothermal gradient of 0.033°C/m and a surface temperature of 20°C. The resulting average temperature in the aquifer is 53.6°C, which yields a maximum ΔT = -23.6°C. This temperature differential is quite low compared to ΔT = -51°C at Cranfield [11] and ΔT = -45°C at In Salah [9, 10]. Pore water pressure is initially hydrostatic and the stress state is calculated according to Equation (10) (Table 2). The *y*-direction of the model coincides with the vertical and the *z*-direction with the out-of-plane direction, which corresponds to the minimum effective stress.

To minimize boundary effects, we set the outer boundary 5 km away from the injection well. Furthermore, the system is only allowed to deform vertically as it is mechanically constrained at all boundaries except over the top of the caprock. Properties of both sandstone and shale are given in Table 3. Shales are assumed to be low permeable, isotropic and homogeneous rocks, with a high capillary entry pressure to ensure initial integrity of the capillary barrier across the caprock.

Table 2. Initial conditions for the geologic storage system

Location	Depth [m]	σ_x [MPa]	σ_y [MPa]	σ_z [MPa]	p_w [MPa]	T [C]
Top of the caprock	914.4	15.56	23.75	15.56	9.41	50
Caprock-aquifer interface	1014.4	17.26	26.35	17.26	10.44	53.28
Aquifer-baserock interface	1034.4	17.6	26.87	17.6	10.65	53.94
Bottom of the baserock	1134.4	19.3	29.47	19.3	11.7	57.22

To simulate non-isothermal CO_2 injection in deformable porous media we use the finite element code CODE_BRIGHT [18] extended for non-isothermal CO_2 injection [5, 16]. A modified version of the Redlich-Kwong equation of state is implemented to calculate thermodynamic properties of CO_2 [19], while CO_2 viscosity is calculated using the polynomial relationship proposed by Altunin and Sakhabetdinov [20].

The mesh of the model is made of structured elements (quadrilaterals), which gradually increase in size away from the injection well. Cell width size ranges from 0.3 m, near the wellbore, to 120 m far away from it; whereas cell height ranges from 0.5 m to 26 m. Elements are exponentially concentrated near the caprock-aquifer interface, to avoid convergence issues over the region of interest, as well as to capture physics of thermal stress reduction over time close enough to the caprock-aquifer interface from above (shale) and below (reservoir.)

Table 3. Rock properties implemented in the THM simulation case study

Property	Reservoir	Shale
Permeability, k [m^2]	10^{-13}	10^{-18}
Relative permeability to water, k_{rw} [−]	S_w^3	S_w^6
Relative permeability to CO_2, k_{rc} [−]	S_c^3	S_c^6
Gas entry pressure, p_c^o [MPa]	0.02	0.6
van Genutchen, m [−]	0.8	0.5
Reference porosity, ϕ_0 [−]	0.1	0.01
Young's Modulus, E [GPa]	10	5
Poisson Ratio, ν [−]	0.3	0.3
Thermal conductivity, λ [W/m-k]	2.4	1.5
Reference solid density, ρ_{s0} [kg/m^3]	2650	2650
Solid specific heat capacity, c_p [J/kg-K]	874	874
Linear thermal expansion coefficient, α_T [C^{-1}]	10^{-5}	10^{-5}

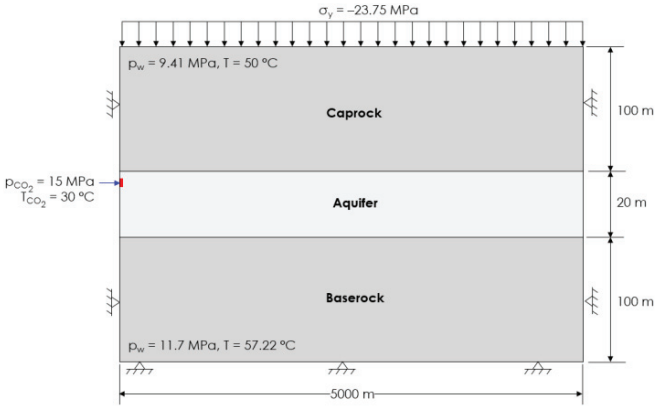

Fig. 3—Schematic representation of the geologic storage system used in this study.

4. Results

Numerical simulation results show that the CO_2 saturation front moves much faster than the temperature front. While the CO_2 plume reaches near 1700 m after 10 years of injection (Fig. 4), the temperature front advances only 50 m (Fig. 5). Thus, thermal stress reduction is localized near the injection well. Fig. 5 shows that tensile stresses are developed inside the aquifer in the cooled region (positive values of the minimum effective stress). Thus, the aquifer indeed fractures near the injection well due to thermal effects.

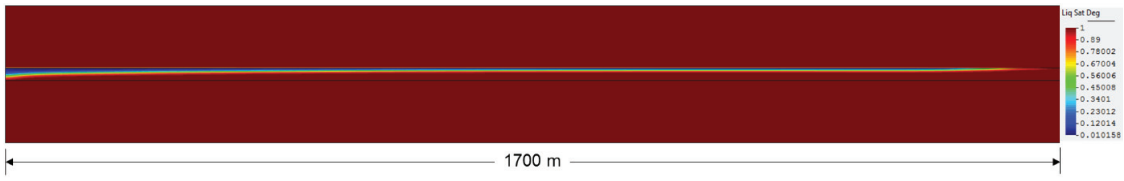

Fig. 4—CO_2 saturation plume reaches 1700 m after 10 years of injection.

Cold CO_2 injection brings along another process relevant to this analysis: stress redistribution. As stresses are reduced in all directions due to rock cooling effects, stress state of the rock must adjust for these changes to attain mechanical equilibrium, as stated by Equation (4). The reason lies in the strain dependency on pressure and temperature (c.f. Equation 5), so that both reservoir and shale layers deform due to ΔT (CO_2 is colder than the interstitial fluid) as well as Δp (CO_2 injection pressure is higher than the in-situ hydrostatic pressure) (Fig. 6). This stress redistribution causes an increase in horizontal stresses in the lower portion of the caprock that compensates for the reduction in the vertical stress within the reservoir. From Fig. 7 it can be seen that the minimum horizontal effective stress exhibits a significant increase thoroughly, with exception of the region inside the aquifer located near the injection well. This effect is pronounced at early times of injection, but progressively dissipates. This progressive dissipation favors the occurrence of hydraulic fracturing conditions in the lower portion of the caprock in the long-term.

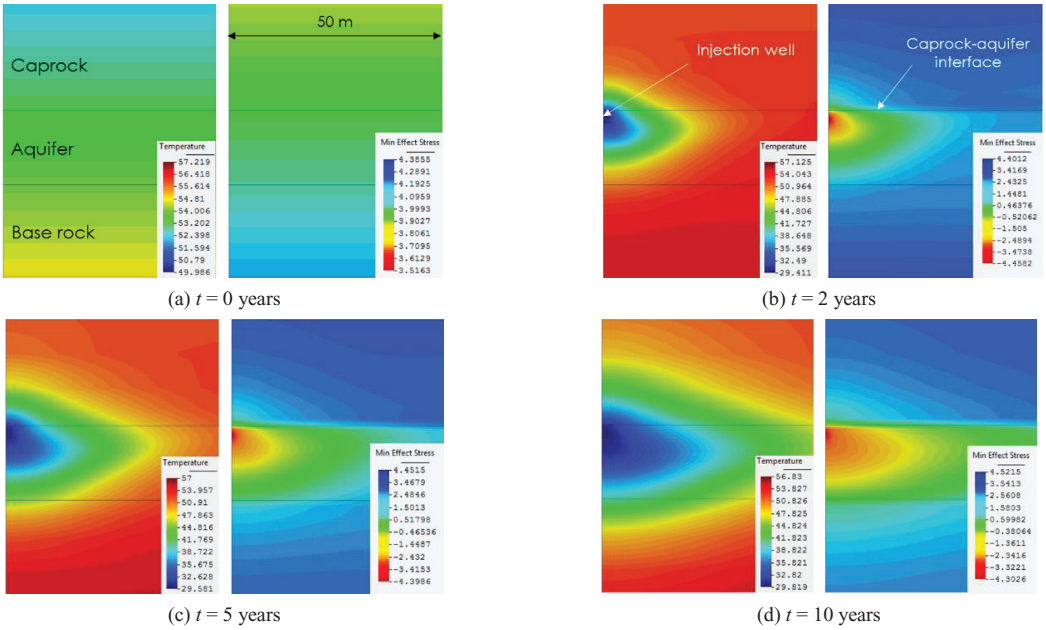

(a) $t = 0$ years (b) $t = 2$ years

(c) $t = 5$ years (d) $t = 10$ years

Fig. 5—Temperature front travels over 50 m after 10 years of CO_2 injection. $\sigma'_h \leq 0$ indicates hydraulic fracturing (per CODE_BRIGHT sign convention, tension is positive). Hence, fracturing occurs within the region with the largest drop in temperature (blue region within the temperature distribution). Temperature is in ºC and stress in MPa.

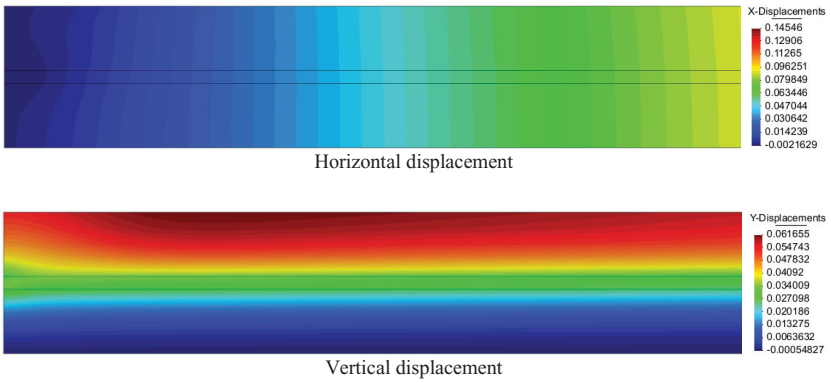

Horizontal displacement

Vertical displacement

Fig. 6—Horizontal and vertical displacements (in m) due to overpressure and cooling effects over $L = 1000$ m after $t = 5$ years of CO_2 injection.

Fig. 7 summarizes the minimum horizontal effective stress profile at various distances away from the injection well. Following the tensile failure criterion (cf. Equation (12)), we can conclude that hydraulic fracturing takes place within the aquifer. To assess the actual horizontal reach of the fracture through the caprock-aquifer interface we apply the same analysis over a distance of 50 m. We estimate that the fracture has a maximum length of 40 m after 10 years of cold CO_2 injection (Fig. 8a). Likewise, we analyze changes in the minimum horizontal effective stress distribution few meters above and below the caprock-aquifer interface. We find that the fracture actually propagates vertically through the caprock-aquifer interface; however, its height is roughly 1 m inside the caprock (Fig. 8b). This is beneficial from the point of view of containment of CO_2 inside the storage formation, but limits the efficiency of the proposed CCUS method, at least for the injection time considered here, i.e., 10 years. Gor et al. [8] found that tensile stresses would appear in the lower portion of the caprock at In Salah after 12 years of cold CO_2 injection. Thus, a higher temperature difference and/or longer injection time are likely to yield tensile stresses in the lower portion of the caprock.

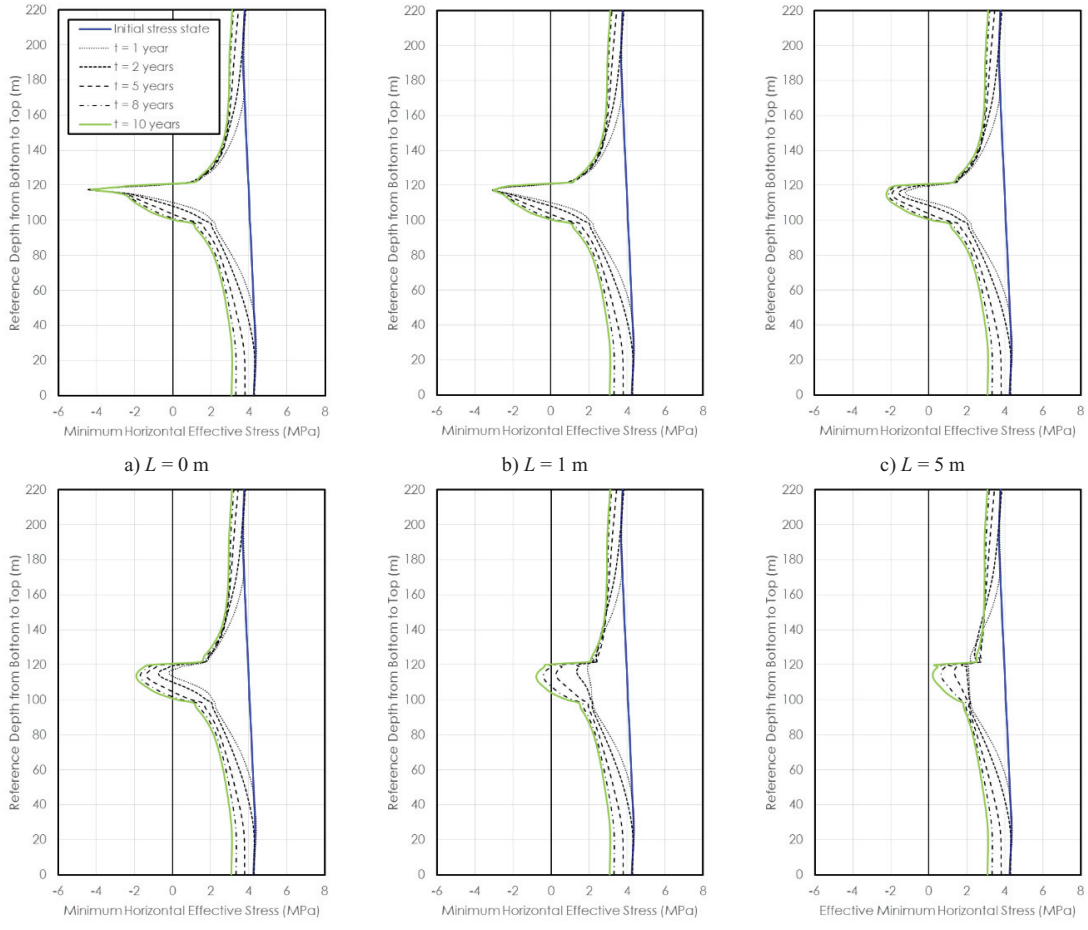

a) L = 0 m b) L = 1 m c) L = 5 m

d) L = 10 m e) L = 30 m f) L = 50 m

Fig. 7—Minimum horizontal effective stress distribution at several distances away from the injection well. The aquifer is located between D = 100 and 120 m. $\sigma'_h \leq 0$ indicates mechanical failure of the rock.

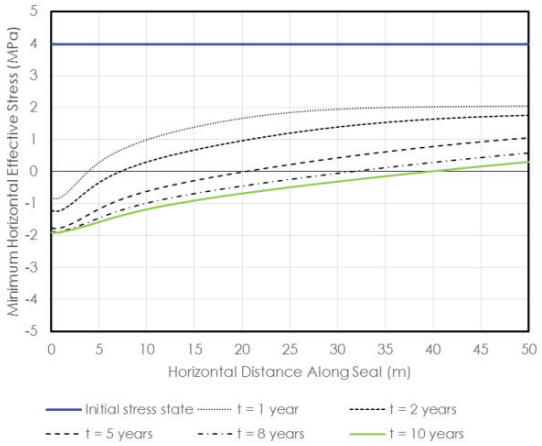

a) minimum horizontal effective stress along the caprock-aquifer interface

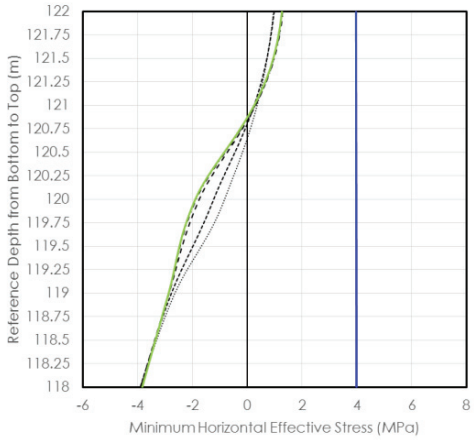

b) detailed minimum horizontal effective stress distribution near the caprock-aquifer interface (D = 120 m)

Fig. 8—Minimum horizontal effective stress distribution along a) caprock-aquifer interface (horizontal), b) aquifer and shale (vertical)

For the simulated case, hydraulic fracturing conditions do not penetrate much into the caprock. However, for caprocks with a higher thermal conductivity or lower heat storage capacity, cooling, and thus hydraulic fractures, may penetrate deeper into shale. While drilling a horizontal well through short fractures in the shale play may not be technically possible, there is still the chance to use the horizontal well originally used for CO_2 injection. In any case, the fracture should be filled with proppant at some point during the injection process aiming to keep it open so production operations would not be jeopardized with fluid pressure falling below the effective minimum in-situ horizontal stress once the lower portion of the caprock starts to warm up.

5. Conclusions

The impact of cold CO_2 injection into a deep saline aquifer overlaid and underlain by shale layers has been analyzed using a thermo-hydro-mechanical modeling approach by means of a finite element code. Numerical simulation results show that hydraulic fracturing can occur due to thermal stress reduction near the injection well. We find that the regions where the minimum horizontal effective stress reduces the most and the cooling effect is the largest coincide. Hydraulic fractures reach a considerable horizontal distance away from the injection point. However, they do not significantly grow inside the shale for the simulated injection time. Fractures merely propagate 1 m through the organic-rich shale after 10 years of injection. Thus, it seems more convenient to produce hydrocarbons through the injection well than drilling a new horizontal well crossing the formed fractures in the lower portion of the caprock. To obtain the maximum benefit of the proposed CCUS method, CO_2 injection should be maintained as long as possible to maximize the penetration depth of cooling-induced hydraulic fractures into organic-rich shales. The production of hydrocarbons at the end of the CO_2 storage project will partly compensate the costs of CCS operations.

Acknowledgements

This study was partially supported by the Louisiana Board of Regents — Research Competitiveness Subprogram (RCS) under contract #43950. V.V. acknowledges financial support from the “TRUST" project (European Community's Seventh Framework Programme FP7/2007-2013 under grant agreement n 309607) and from “FracRisk" project (European Community's Horizon 2020 Framework Programme H2020-EU.3.3.2.3 under grant agreement n 640979).

References

[1] J. David and H. Herzog, "The Cost of Carbon Capture," *Energy*, pp. 13–16, 2000.

[2] J. B. Randolph and M. O. Saar, "Coupling carbon dioxide sequestration with geothermal energy capture in naturally permeable, porous geologic formations: Implications for CO_2 sequestration," *Energy Procedia*, vol. 4, no. May, pp. 2206–2213, 2011.

[3] M. H. Holtz, P. K. Nance, and R. J. Finley, "Reduction of greenhouse gas emissions through CO_2 EOR in Texas," *Environ. Geosci.*, vol. 8, no. 3, pp. 187–199, 2001.

[4] L. Paterson, M. Lu, L.D. Connell, and J. Ennis-King, "Numerical modeling of pressure and temperature profiles including phase transitions in carbon dioxide wells, " *SPE Annual Technical Conference and Exhibition*, Denver, 21-24 September, 2008.

[5] V. Vilarrasa, S. Olivella, J. Carrera, and J. Rutqvist, "Long term impacts of cold CO_2 injection on the caprock integrity," *Int. J. Greenh. Gas Control*, vol. 24, pp. 1–13, 2014.

[6] S. Goodarzi, A. Settari, M.D. Zoback, and D.W. Keith, "Optimization of a CO_2 storage project based on thermal, geomechanical and induced fracturing effects, " *Journal of Petroleum Science and Engineering*, vol. 134, pp. 49–59, 2015.

[7] M. Preisig and J. H. Prévost, "Coupled multi-phase thermo-poromechanical effects. Case study: CO_2 injection at In Salah, Algeria," *Int. J. Greenh. Gas Control*, vol. 5, no. 4, pp. 1055–1064, 2011.

[8] G. Y. Gor, T. R. Elliot, and J. H. Prévost, "Effects of thermal stresses on caprock integrity during CO_2 storage," *Int. J. Greenh. Gas Control*, vol. 12, pp. 300–309, 2013.

[9] R. C. Bissell, D. W. Vasco, M. Atbi, M. Hamdani, M. Okwelegbe, and M. H. Goldwater, "A full field simulation of the in Salah gas production and CO_2 storage project using a coupled geo-mechanical and thermal fluid flow simulator," *Energy Procedia*, vol. 4, pp. 3290–3297, 2011.

[10] J. Rutqvist, "The Geomechanics of CO_2 Storage in Deep Sedimentary Formations," *Geotech. Geol. Eng.*, vol. 30, no. 3, pp. 525–551, 2012.

[11] S. Kim and S. A. Hosseini, "Above-zone pressure monitoring and geomechanical analyses for a field-scale CO_2 injection project in Cranfield, MS," *Greenh. Gases Sci. Technol.*, vol. 4, no. 1, pp. 81–98, 2014.

[12] T. R. Elliot and M. A. Celia, "Potential restrictions for CO_2 sequestration sites due to shale and tight gas production," *Environ. Sci. Technol.*, vol. 46, no. 7, pp. 4223–4227, 2012.

[13] J. Bear, *Dynamics of Fluids in Porous Media*. Courier Corporation, 1971.

[14] C. R. Faust and J. W. Mercer, "Geothermal reservoir simulation: 1. Mathematical models for liquid-and vapor-dominated hydrothermal systems," *Water Resour. Res.*, vol. 15, no. 1, pp. 23–30, 1979.

[15] P. Segall and S. D. Fitzgerald, "A note on induced stress changes in hydrocarbon and geothermal reservoirs," *Tectonophysics*, vol. 289, no. 1, pp. 117–128, 1998.

[16] L. Lake, *Petroleum Engineering Handbook*. Richardson, TX: Society of Petroleum Engineers, 2007.

[17] V. Vilarrasa, D. Bolster, S. Olivella, and J. Carrera, "Coupled hydromechanical modeling of CO_2 sequestration in deep saline aquifers," *Int. J. Greenh. Gas Control*, vol. 4, no. 6, pp. 910–919, 2010.

[18] S. Olivella, A. Gens, J. Carrera, and E. E. Alonso, "Numerical formulation for a simulator (CODE_BRIGHT) for the coupled analysis of saline media," *Eng. Comput.*, vol. 13, no. 7, pp. 87–112, 1996.

[19] N. Spycher and K. Pruess, "CO_2-H_2O Mixtures in the Geological Sequestration of CO_2. II. Partitioning in Chloride Brines at 12-100°C and up to 600 bar," *Lawrence Berkeley Natl. Lab.*, 2004.

[20] V. V Altunin and M. A. Sakhabetdinov, "Viscosity of liquid and gaseous carbon dioxide at temperatures 220-1300 K and pressure up to 1200 bar," *Teploenergetika*, vol. 8, pp. 85–89, 1972.